Development of novel miniature microwave discharge thruster

IEPC-2015-245／ISTS-2015-b-245

Presented at Joint Conference of 30th International Symposium on Space Technology and Science
34th International Electric Propulsion Conference and 6th Nano-satellite Symposium,
Hyogo-Kobe, Japan
July 4 – 10, 2015

Koichi Ushio[1], Yuji Toyoda[2] Naoji Yamamoto[3], Taichi Morita[4] and Hideki Nakashima[5]
Kyushu University, Fukuoka, Japan

Abstract: We have been developing a novel miniature microwave discharge plasma thruster for micro satellites. The target of power consumption, thrust and specific impulse are 10 W, 1 mN and 1000 sec, respectively. We fabricated the thruster and estimated the thrust from the measured ion beam current and ion energy distribution function using an ion collector and a retarding potential analyzer, respectively. Several parameters, antenna configuration, the length of discharge chamber, configuration and magnetic field strength, were optimized for the improvement of the thrust performance. The overall thrust was estimated to be 81.5 μN at incident microwave power of 10 W, mass flow rate of 82 μg/s.

Nomenclature

e	=	electronic elementary quality, C
F	=	thrust, N
I_b	=	ion beam current, A
I_c	=	ion current into the collector inside a retarding potential analyzer, A
I_{c0}	=	I_c when $V_{sw} = 0$, A
$\dot{m}$	=	mass flow rate of propellant, kg/s
m	=	ion mass, kg
L_c	=	length of the central yoke, m
V_i	=	ion velocity, m/sec
V_{sw}	=	ion retarding grid applied voltage, V

I. Introduction

IN these days, launches of micro satellites is increase. 90% of the satellites launched in 2013 is 50 kg class or less, since micro satellites have low cost and short development time[1]. Participation in space utilization becomes more easier for academy, venture company and the developing countries[2,3]. Launch of micro satellites is more frequent than big satellites because micro satellites can be launched as piggyback satellite[4,5].

Though the ability of micro satellite is restricted compared to large satellites, micro satellite can get the capacity competitive with the large satellites if they adopt formation flight and constellation[6,7]. These also have other advantages that the risk of failure can be reduced and supplement of extra function is easy. Most of micro satellites

[1] Graduate student, Department of Advanced Energy Engineering Science, ushio@aees.kyushu-u.ac.jp.
[2] Graduate student, Department of Advanced Energy Engineering Science, toyoda@aees.kyushu-u.ac.jp.
[3] Associate Professor, Department of Advanced Energy Engineering Science, yamamoto@aees.kyushu-u.ac.jp.
[4] Assistant Professor, Department of Advanced Energy Engineering Science, morita@aees.kyushu-u.ac.jp.
[5] Emeritus Professor, Department of Advanced Energy Engineering Science, nakasima@aees.kyushu-u.ac.jp.

have no thruster, since there is little space to install thrust systems and small solar array will not allow the large power consumption of thruster.

Some micro satellites have a thruster like “Hodoyoshi-3&4” and “PROCYON” in these days[8,9]. Since thruster enable microsatellites to perform more advanced mission. The thrusters offer the opportunity to the micro satellites orbit transfer or orbit keping. One of the advanced mission is a super low altitude keeping. The super low altitude satellite flights at the super low altitude of about 180~250 km, so this satellites can observe with high resolution and reduce emission power of active sensors[10,11]. The super low altitude satellites can minimize the device for observation and decrease the power consumption for sensor. These satellites have to compensate the drag by using the thruster. The electric propulsion is suitable for compensation of the drag because the thruster should be operated while orbit keeping and the mounted propellant mass is restricted due to the small room. “GOCE”, which mass is 1100 kg, used two 20 mN class ion thrusters[12]. “SLATS” will also use an ion thruster. Therefore, we have been developing the thruster for a 50 kg class micro super low altitude satellite whose size is 0.1 m×0.1 m×0.5 m. The required thrust, specific impulse are 1 mN and 1000 sec, respectively within the total power consumption in 10 W. We adopted a novel concept of thruster, using a microwave discharge and fabricated and evaluated the thrust performance of it.

II. Novel microwave discharge thruster

A. A novel principle of ion acceleration

Figure 1 shows the schematic of ion acceleration mechanism of this thruster. The plasma is generated by microwave discharge. Electrons is trapped in a magnetic tube[13], where is the area between magnetic mirrors. Electrons gain energy from the microwaves and they collide propellant particles and the propellant atoms are ionized. The ions are accelerated by the potential difference between the plasma inside the thruster and the space, if the discharge chamber is kept the potential same as the space potential. High energetic electrons can also go out to downstream with ions against the potential difference. These electrons and ions outside the thruster are neutralized; it does not need a neutralizer. Therefore, this thruster is very simple and small, and this thruster can operate in low power consumption.

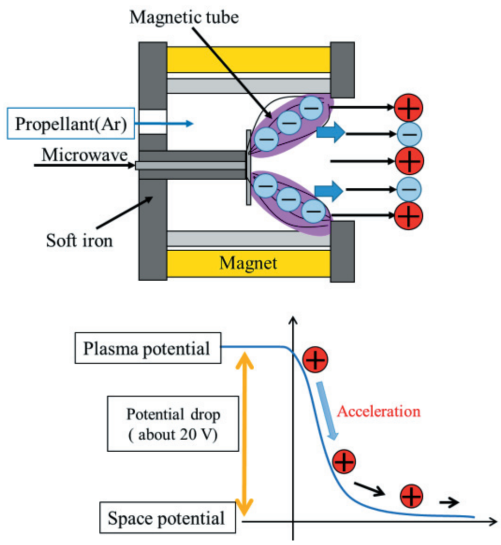

Fig.1 Principle of ion acceleration

III. Experimental setup

A. Miniature microwave discharge thruster

Figure 2 shows the appearance a of the microwave discharge thruster. We use two thrusters, one is 50 mm×50 mm×27 mm and the other is 50 mm×50 mm×53.5 mm. Figure 2(b) shows the parts assembly of the short one. Some Sm-Co magnets surround the discharge camber and these are put between the yokes made of soft iron. The magnet size is 4 mm×4 mm×12 mm. The inner diameter of the discharge chamber is 21 mm and the height of that is 12 mm. There are a spacer and an orifice plate in front of the front yoke. The diameter of the spacer and the orifice is 21 mm and 12 mm respectively. The sickness of the spacer and orifice is 4 mm and 2 mm respectively. The antenna is made of molybdenum. The antenna has the size inscribed the circle with a diameter of 9 mm and a thickness of 1 mm. The propellant is argon.

Figure 2(d) shows the parts assembly of the long one. The discharge chamber is extended to 33 mm. The magnets and the central yoke is extended to fit the discharge chamber. The back yoke become large from 35 mm×35 mm×3 mm to 50 mm×50 mm×12 mm. The others are the same as short one’s.

Figure 3 shows the magnetic field distribution of two types at the number of magnet of 9(short type) and 14(long type). Magnetic field strength inside the discharge chamber can be changed by changing the number of magnets.

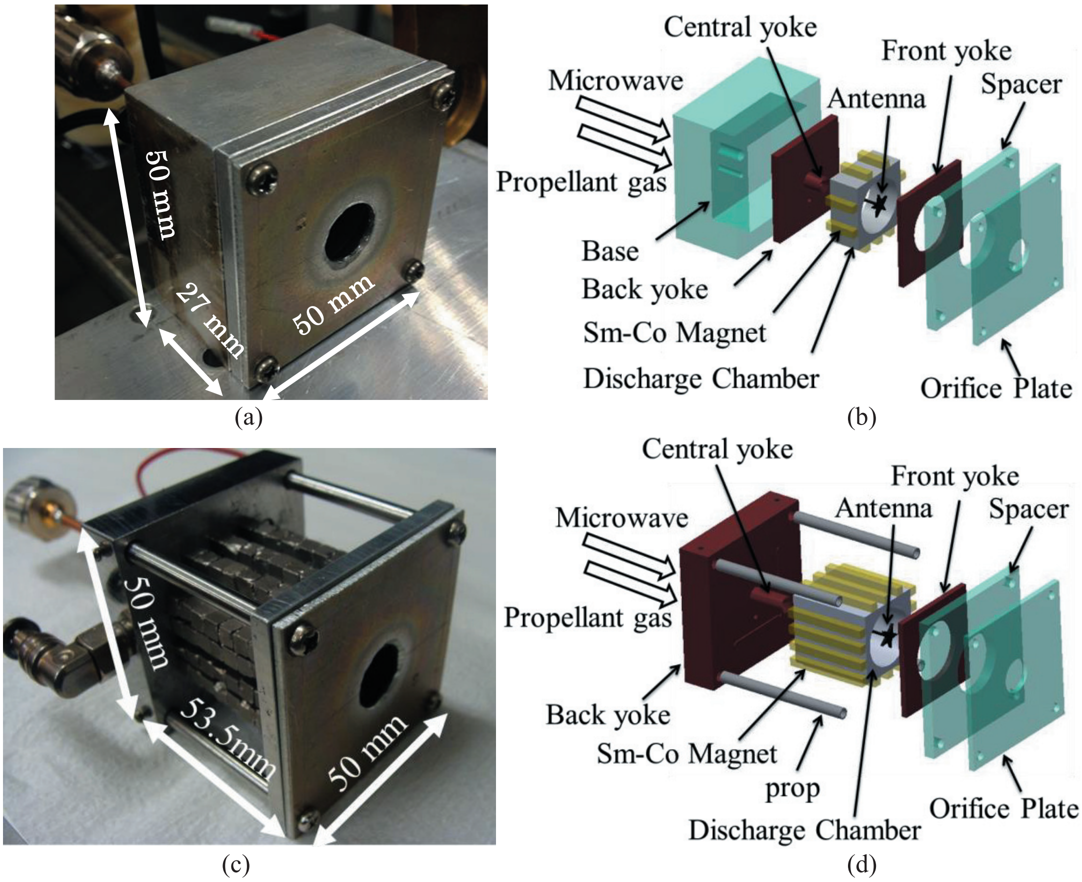

Figure 2. Appearance of the thruster, (a)photo of short type (b)parts assembly of short type,(c) photo of long type(parts assembly of the long type

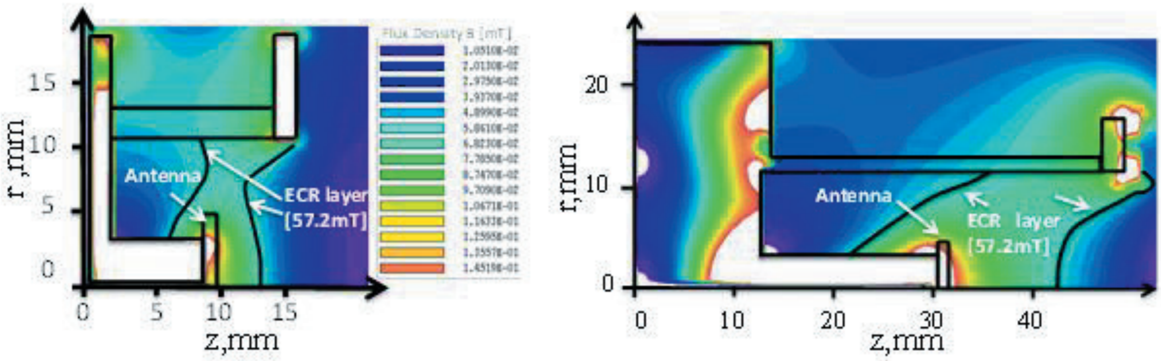

(a) (b)

Figure 3. Magnetic field distribution for each discharge chamber (a) short type, (b) long type

B. Ion beam measurement

The performance of this propulsion is evaluated by measuring ion beam current and ion energy distribution function (IEDF). For estimation of the thrust, the following equation was used[14].

$$F = \dot{m}V_{\mathrm{i}} = \frac{m_{\mathrm{i}} I_b V_{\mathrm{i}}}{e} \qquad (1)$$

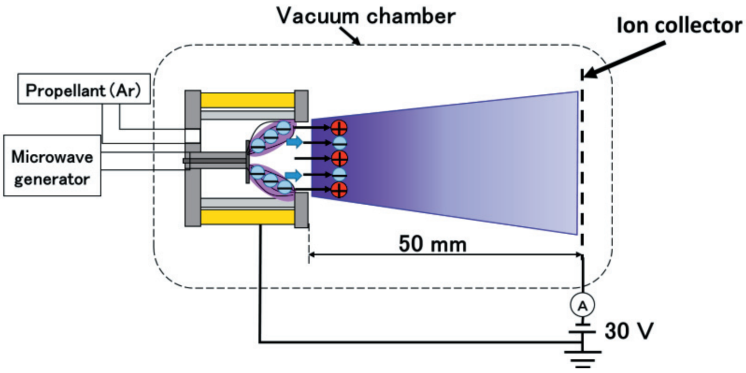

Figure 4. Schematic of the measurement of ion current

Figure 4 shows the schematic of the experiment. The diameter and length of vacuum is 1.0 m and 1.2m respectively. The pumping system consists of a mechanical booster pump (pumping speed 1.0×10^{-1} m^3/sec) assisted by a rotary pump (pumping speed 2.7×10^{-2} m^3/sec) and turbo molecular pumps (pumping speed 2.2 m^3/sec). The ion collector is applied -30 V to reflect the electrons and the ion current is saturated at -30 V. The distance between the collector and thruster is 50 mm. The chamber baseline pressure is below 5.7×10^{-4} Pa. The back pressure is 1.4×10^{-2} Pa at argon mass flow rate of 41 µg/s. Microwave is generated by a generator and the frequency is 1.6 GHz, it goes to the discharge chamber through the coaxial cable after amplification.

C. Measurement of the ion energy

The energy of the exhausted ions was measured by using Retarding Potential Analyzer (RPA). RPA consists of four grids and one collector as shown in Fig.5. We measured the collector current while scanning the voltage of Ion Retarding Grid(IRG) from0 to 65 V. Electron Retarding Grid(ERG) and Secondary Electron Suppression Grid(SESG) is applied -40 V. Floating Grid(FG), ERG and SESG is 200 mesh/inch, IRG is 400 mesh/inch. FG is the three piled. This is to prevent the ionization of the neutral particles and space charge limitation by decrease the amount of the ion and neutral particles flow into RPA. IRG has small mesh to prevent generation of the lower voltage area than applied voltage in the mesh. The following equations were used to get the IEDF[15].

$$E_{\mathrm{sw}} = eV_{\mathrm{sw}} \tag{2}$$

$$\mathrm{f(E)} = -\frac{1}{I_{\mathrm{c0}}}\frac{dI_{\mathrm{c}}}{dE_{\mathrm{sw}}} \tag{3}$$

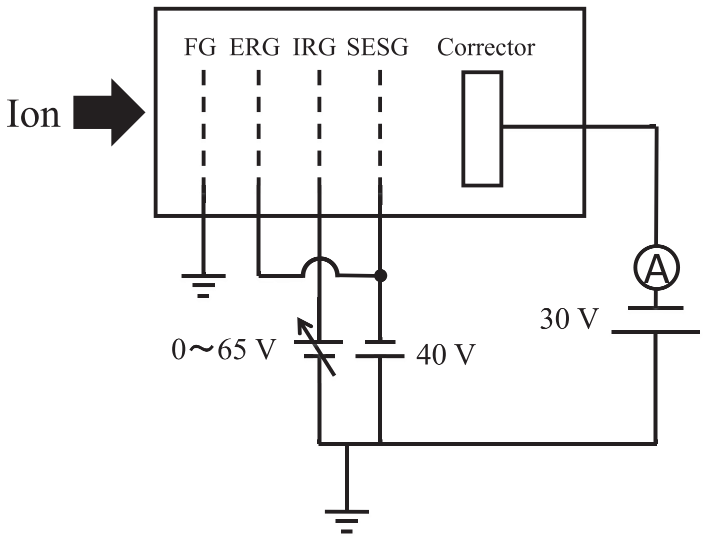

Figure 5. Schematic of retarding potential analyzer.

IV. Experimental results

A. Dependence on the antenna configuration

Our previous study showed that the shape of antenna affected the thrust performance in ion thruster[16]. Figure 6 shows the appearance of antenna. The star antenna showed better performance than other antenna shapes in ion thruster. The L shape antenna is used for microwave discharge neutralizer[17]. The circle antenna has most big surface area. The result is shown in Fig.7, at argon mass flow rate of 82 μg/sec, and the number of magnets of 9. In this experiments, data is the average over the three experiments and the standard deviation of the currents is less than 0.1 mA, so the error is so small and it doesn't see in the graph.

The star antenna shows the best performance and circle antenna shows the performance which is next to star. This would be due to the surface recombination depending on the surface area. Ion beam current was very low, it is 1~2 mA with L shape antenna. It is seemed that plasma was not uniform and the entire magnetic tube can't be efficiently utilized. This results show that the antenna and magnetic tube should touch in the wide area.

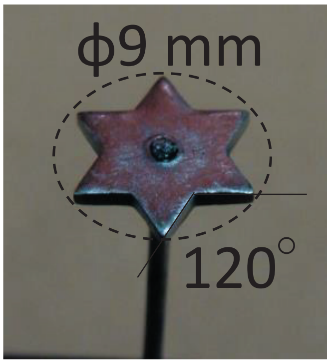

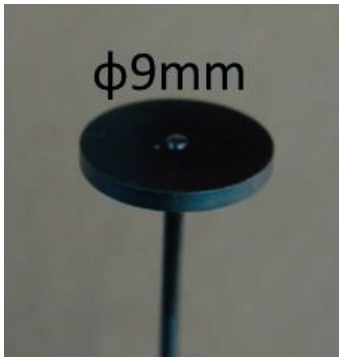

Figure 6. Appearance of antenna

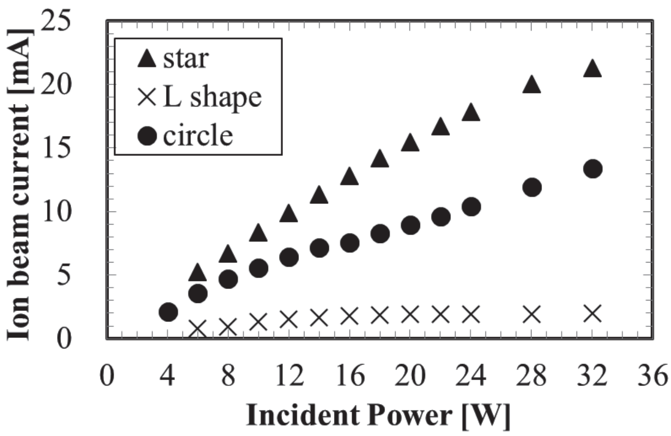

Figure 7. Dependence of the ion beam current on the antenna configuration

B. Extension of the discharge chamber

It is necessary to increase the chance of the plasma generation, so the length of the discharge chamber was extended in order to expand the volume for plasma generation. Magnetic tube has the important role on the plasma generation[18]. The length of the extended discharge chamber is 33 mm and the length of the central yoke is also extended from 7 mm to 19 mm in order to keep the ratio between the length of the discharge chamber and the central yoke. The ion beam current was investigated for the several number of the magnets. Figure 8 (a), (b), (c), (d) shows the magnetic field distributions with the number of magnets of 10, 12, 14 and 16 respectively. The ECR become far away from the antenna with increase in the number of magnets. The other experimental conditions is same as the experiment on above section.

Figure 9 shows the results of the experiments. The ion beam current increases with the increase in the number of magnets. This is because the plasma confinement was improved with the increase in the number of magnets. However, the ion beam current decreases from 7.6 mA to 6.2 mA when the number of magnets was changed from 14 to 15. It is seemed that the ECR layer is too far from antenna and the coupling between microwave and plasma worsened. Therefore, the ion beam current was maximum when the number of magnet is 14 by tradeoff of the plasma confinement and the coupling of plasma and microwave.

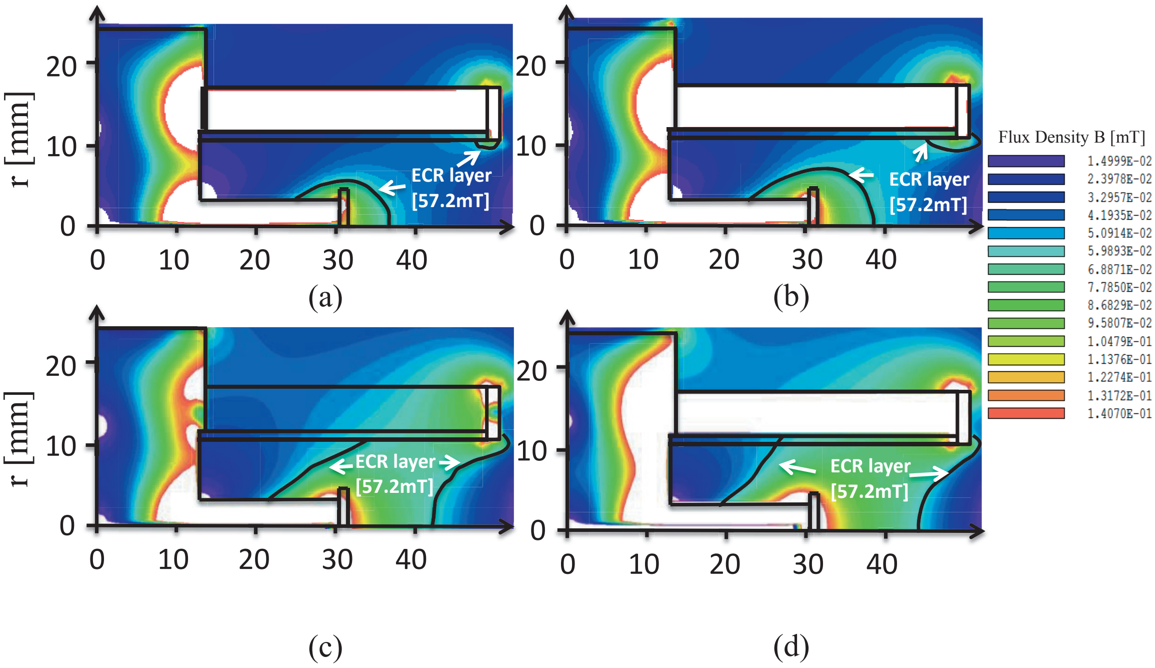

Figure 8. Magnet field distribution with the number of magnet is (a)10, (b)12, (c)14, (d)16

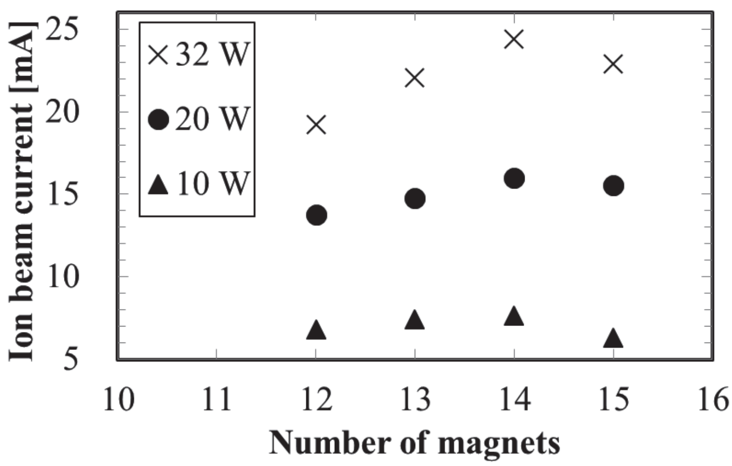

Figure 9. Dependence of the ion beam current on the number of magnet

The IEDF was measured for the two discharge chambers. The number of magnets for two thrusters are 9 and 14, respectively. Star antenna was used. The other conditions is same as previous experiment on above section. The measured IEDF is shown in Fig.10. The average ion energy is 16.8 eV and 13.7 for the length of discharge chamber is 12 mm and 33mm respectively at incident power 10 W. The ion energy decrease with the expansion of the discharge chamber. This is indicate that the plasma potential downed. This is caused by the fall of the electron temperature by the decrease of the frequency that the electron approach near the antenna, it is caused by expansion of magnetic tube. IEDF is not symmetry and biased to the low energy side. This is caused by charge exchange collision occur until ion reach RPA from thruster. Therefore, the average ion energy might be underestimate.

Figure 11 shows the ion beam current when the discharge chamber is 12 mm and 33 mm. The difference between two conditions is small, it is about 0.7 mA at incident power of 10 W, but it becomes 3 mA at incident power of 32 W. This is because the electron temperature increased with increase in the incident power, and mean free pass became long and the optimum length of the magnetic tube was extended. These results indicate that there is the best length of discharge chamber for each incident power.

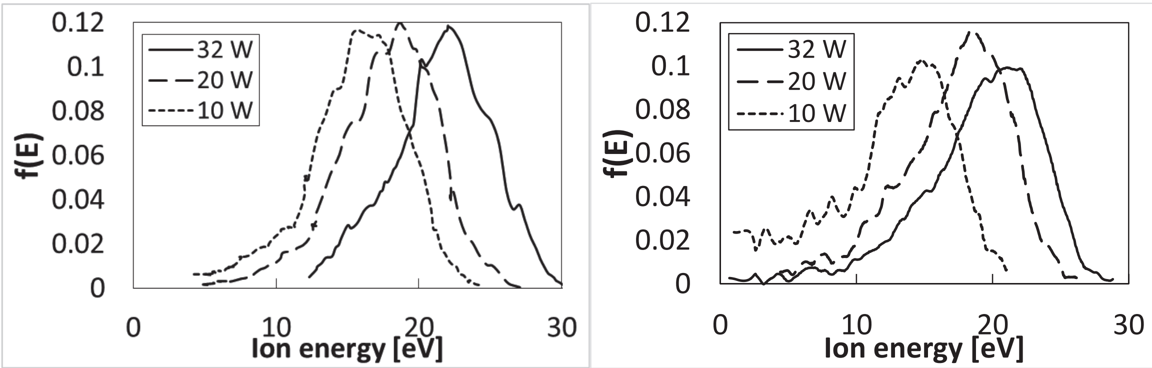

(a) (b)

Figure 10. IEDF for the length of discharge chamber is (a)12 mm, (b)33 mm.

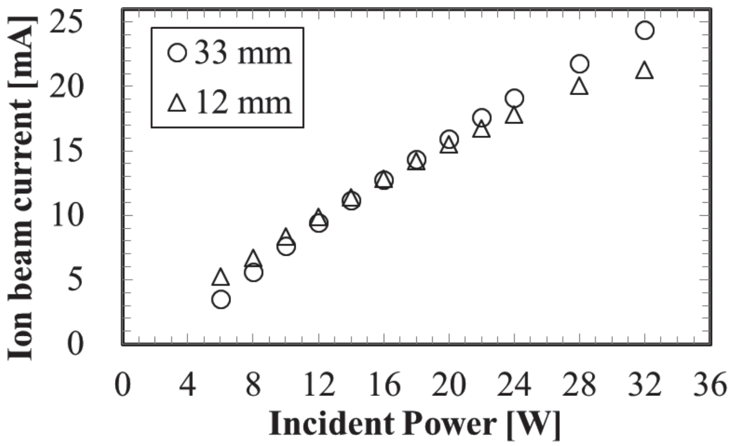

Figure11. Ion beam current for the length of discharge chamber is 12 mm, 33 mm

C. Dependence of the length of the central yoke

Ion beam current is measured for the several length of the central yoke (L_c). The magnetic field distribution is changed by changing of the length of the central yoke. Figure 12 shows magnetic field distributions for the several length of the central yoke when the number of magnets is 9. The length of discharge chamber is 12 mm, mass flow rate is 82 μg/sec and 41 μg/sec, the other conditions is same as previous experiment on above section. Figure 13 and Fig.14 shows the ion beam current for four lengths of the central yoke, 3 mm, 5 mm, 7 mm, 9 mm at the number of magnets of 11, 10, 9, 9, respectively and argon mass flow rate of 82 μg/sec and 41 μg/sec. These number of magnets are optimized for the best performance. The ion beam current was 12.7 mA and 4.7 mA when the length of the central yoke is 7 mm and 5 mm at mass flow rate of 41 μg/sec and the incident power of 32 W. The ion beam current becomes about three times large if the length of the central yoke changes from 5 mm to 7 mm. However, the difference in the each ion beam currents is small at the mass flow rate of 82 μg/sec. This is because that the frequency of collision is too high and there is no optimum length of magnetic tube. These results indicate that there are the best length of the central yoke for each mass flow rate.

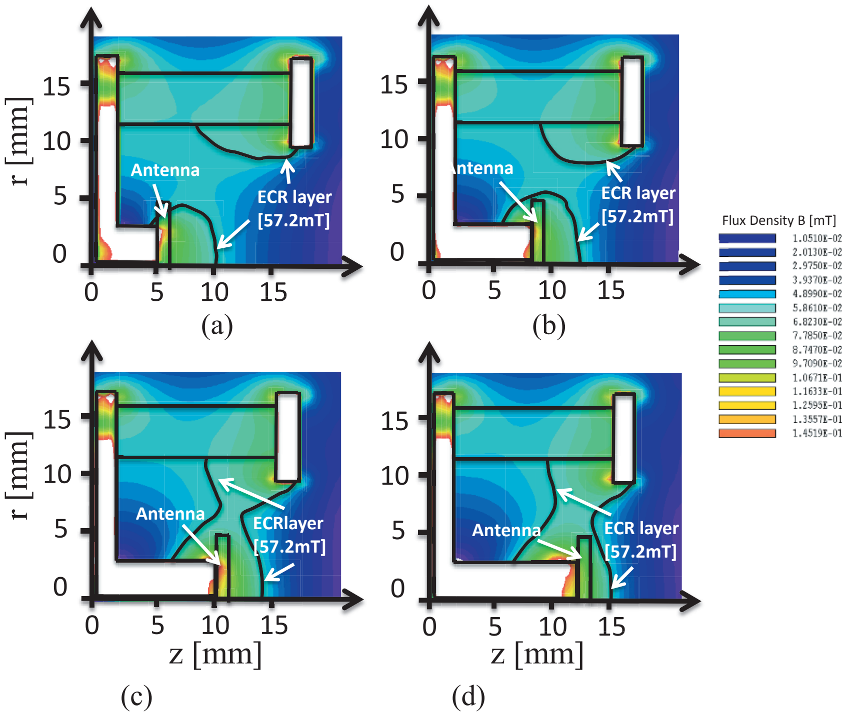

Figure12. Magnetic field distribution with the length of central yoke is (a) 3mm, (b) 5 mm, (c) 7 mm, (d) 9

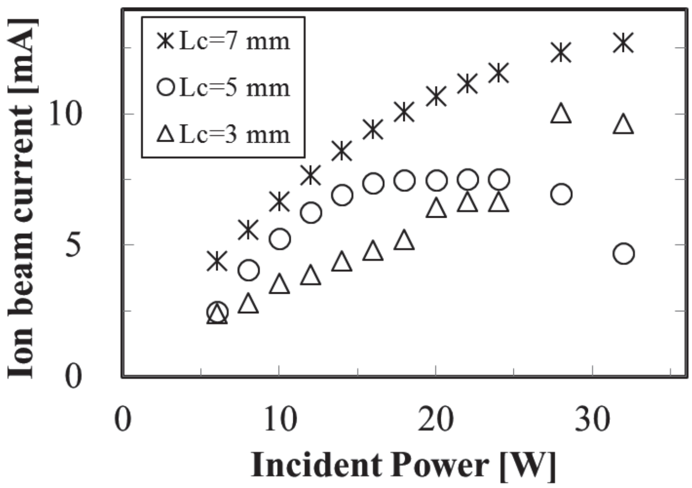

Figure13. Dependence on the length of central yoke for 41 μg/sec

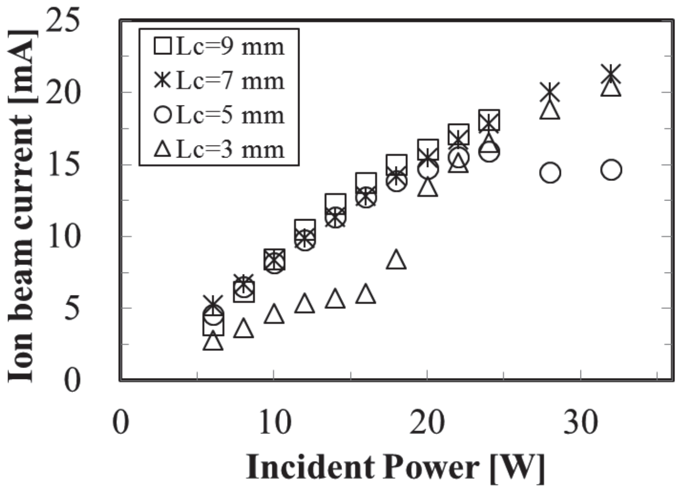

Figure 14. Dependence on the length of central yoke for 82 μg/sec

D. The ion beam current measurement by cylindrical collector

The result of measurement of ion energy distribution function indicated that the ions were scattered by charge exchange collision. It means that the performance can't be evaluated exactly by the ion beam current measurement. The cylindrical collector was used instead of the plate collector in order to collect the scattered ions. Figure 15 shows the appearance of the cylindrical collector. This collector has many holes. The aperture ratio is 48% to prevent the confinement of neutral particles. Figure 16 shows the results of experiments. The ion beam current is 51 mA at incident power 32 W. This shows that about 50% of exhausted ion was scattered by charge exchange collision. Considering the hole of the cylindrical collector, so the measured ion beam current should be compensated. The coefficient of compensation is 1.91, and it is determined by assumption that the rate which ions escape equal to aperture ratio. Table.1 shows the compensated performance. The thrust estimated 81.5 μN when the incident power is 10 W. However, even this performance is 1/10 thrust of objective. This performance might be overestimated by the effect of the confinement of neutral particle and the error of method of the compensation. Therefore, the method which can evaluate the performance exactly is needed.

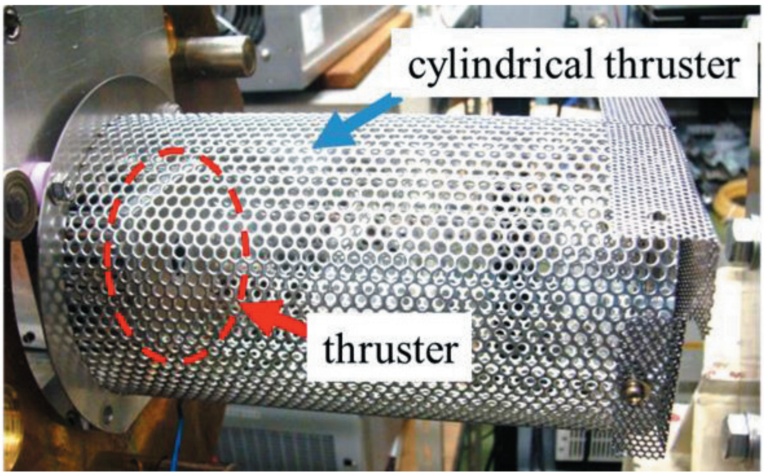

Figure 15. Appearance of cylindrical collector

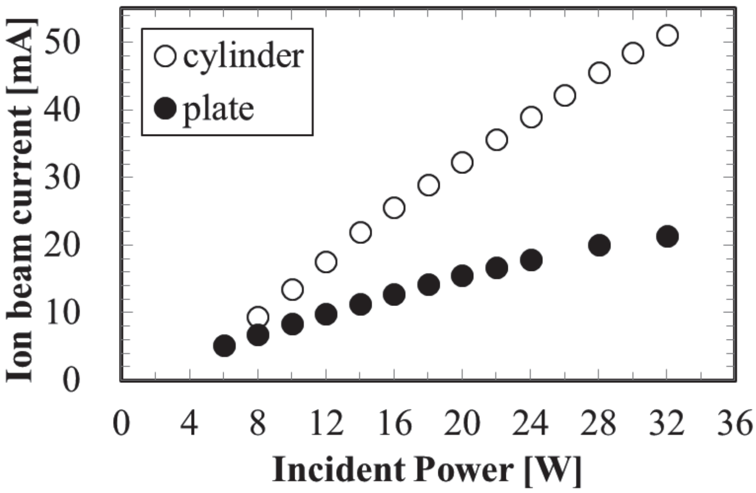

Figure16 Dependence of the configuration of the collector

Table.1 Performance estimated by using cylindrical collector

Incident power	10 W	20 W	32 W
Ion beam current	24.2 mA	66.0 mA	105 mA
Thrust	81.5 μN	250 μN	425 μN
Specific impulse	100 sec	309 sec	523 sec
Propellant utilization	12.1 %	33.0 %	52.6 %

V. Conclusion

We have been developing a novel miniature microwave discharge thruster and investigate the dependency of several parameters on the thrust performance in order to improve the thrust performance. The best antenna configuration is star, because it touches the magnetic tube in wide area and has small area touch the magnetic tube. The length of discharge chamber is expanded from 12 mm to 33 mm and the number of magnets is optimized to 14. However, the ion beam current increased in some condition, but the exhausted ion energy decreased. This is might be caused by decrease in electron temperature. The length of the central yoke was also optimized to 7 mm. The collector configuration is changed from plate to cylinder and the ion beam current become four times. Finally, the performance was estimated that the thrust is 81.5 μN, specific impulse is 100 sec and propellant utilization efficiency is 12.1% when the incident power is 10 W. However, this performance was estimated by using many assumptions. The performance should be evaluated exactly by thrust stand in future.

References

[1]Mitsuteru Kaneoka, "A summary and task of Nano/Micro satellites", *58th Space Sciences and Technology Conference*, JSASS-2014-4035, Tokyo, 2014

[2]Saburo Matunaga, "Dream and reality of Nanosatellites", *International Journal of Microgravity Science Application*. Vol.30 No.3, Saitama, Japan, 2013(136-142). pp.136-142.

[3]Utoro Sastrokusumo, Rudi Lumanto, "LAPAN A2 Micro Satellite and the Need for Rapid Emergency Communication", *29th International Symposium on Space Technology and Science*, 2013-f-40, Tokyo, 2013

[4]Masahiro Yamazaki, "Mission of Piggy –back Satellite SPROUT Launched with ALOS −2", T*he Institute of Electronics, Information and Communication Engineers*, SANE2012−34(2012−6), Tokyo, 2012, pp.77-81

[5]Tsuruda Yoshihiro, Toshiya Hanada, Jozef C. van der Ha, "QSAT: A Low-Cost Design for 50kg Class Piggyback Satellite", *26th International Symposium on Space Technology and Science*, 2008-f-20, Tokyo, 2008.

[6]Isao Kawano, Toru Ymamoto, Shinji Mitani, "Application of formation flying technology to frontier space missions", *The Institute of Electronics, Information and Communication Engineers*, SANE2009 −37(2009−6), Tokyo, 2009. Pp.127-132.

[7]Korehiro Maeda, "Present and future of near earth satellite mission: Applications to Observation and Communication system of small satellites", *The Institute of Electronics, Information and Communication Engineers*, Tokyo, SNE2012-87(2012-10), 2012, pp.173-180.

[8]Yoshihiro Tsuruda, Shinichi Nakasuka, Matsui Masayasu, Ichiro Mase, "Reasonably Reliable System Design and Operation for Twin Satellite: Hodoyoshi-3 & 4", *Proceedings of 58th Space Sciences and Technology Conference,* JSASS-2014-4218, Tokyo, 2014.

[9]Hiroyuki Koizumi, Yusuke Kasagi, Tadashi Inagaki, Hiroki Kawahara, Kazuya Yaginuma, Jun Asakawa, Kimiya Komurasaki, "Development of small propulsion system for nano-satellites and its challenges for the future", *Proceedings of 58th Space Sciences and Technology Conference*, JSASS-2014-4333, Tokyo, 2014

[10]Kazuya Konoue, Shunsuke Imamura, Yohei Satoh, Haruo Kawasaki, Hiroki Kohata, "Development Status of Super Low Altimde Test Satellite "SLATS"", *The Institute of Electronics, Information and Communication Engineers*, Tokyo, 2011, pp.1-5.

[11]Ming Xu, Nan Zhou, "Image Positioning Accuracy Analysis for Super Low Altitude Remote Sensing Satellites", International Journal of Advanced Robotic Systems, Rijeka, Croatia, 2012, Vol. 9, 160.

[12]Neil Wallace, Peter Jameson, Christopher Saunders, Michael Fehringer, Clive Edwards, Rune Floberghagen, "The GOCE Ion Propulsion Assembly – Lessons Learnt from the First 22 Months of Flight Operation", *The 32nd International Electric Propulsion Conference, New York*, IEPC-2011-327, Germany, 2011.

[13]Ikkoh Funaki, Hitoshi Kuninaka, Kyoichiro Toki, "Plasma Characterization of a 10-cm Diameter Microwave Discharge Ion Thruster", J. Propul. Power, Vol.20, No.4, 2004, pp. 718-726.

[14]Kyoichi Kuriki, Yoshihiro Arakawa, *Introduction to Electric Propulsion*, University of Tokyo Press, Tokyo, 2003, pp.99.

[15]B. van Reijen, S. Weis, A. Lazurenko, J. Haderspeck, A. Genovese, and P. Holtmann, "High Precision Thrust Vector Determination through Full Hemispherical RPA Measurements assisted by Angular Mapping of Ion Energy Charge State Distribution", *The 33nd International Electric Propulsion Conference,* IEPC-2013-284. New York, 2013.

[16]Naoji Yamamoto, Hirokazu Masui, Hiroshi Kataharada, Hideki Nakashima, Yoshiyuki Takao, "Antenna Configuration Effects on Thrust Performance of Miniature Microwave Discharge Ion Engine", *Journal of Propulsion and Power*, Vol. 22, No. 4, AIAA, Washington, DC, 2006. pp. 925-928.

[17]Kenichi Kubota, Hiroki Watanabe, Ikkoh Funaki, Naoji Yamamoto, Hideki Nakashima, Takeshi Miyasaka, "Development of Hybrid-PIC Solver for Microwave Neutralizer", *29th International Symposium on Space Technology and Science*, 2013-b-38, Tokyo, 2013.

[18]Satoshi Hosoda, Hitoshi Kuninaka, "The Homeward Journey of Asteroid Explorer "Hayabusa" Powered by the Ion Engines", *J.Plasma Fusion Res*, Vol86,No.5(2010)282-292, Nagoya, Aichi, 2010.